Selective Oxidation of Mn alloyed Steels during annealing prior to galvanizing

Factsage user meeting

18-7-2017

W. Mao and W.G. Sloof

Delft University of Technology

Department of Materials Science and Engineering

Surface and Interface Engineering

Content

- Project background
- Prediction of oxide phases formed upon internal oxidation of Fe-Mn-Cr steel alloys
- Compositional depth profile of internal (Mn,Fe)O in oxidized Mn alloyed steel
- Outlook

1.

Background

Advanced high strength steel (AHSS) in automotive industry

Advantage

- Reduction in body weight, fuel consumption and CO_2 emission

Main drawback

- Low corrosion resistance

Solution

- Hop-dip galvanizing

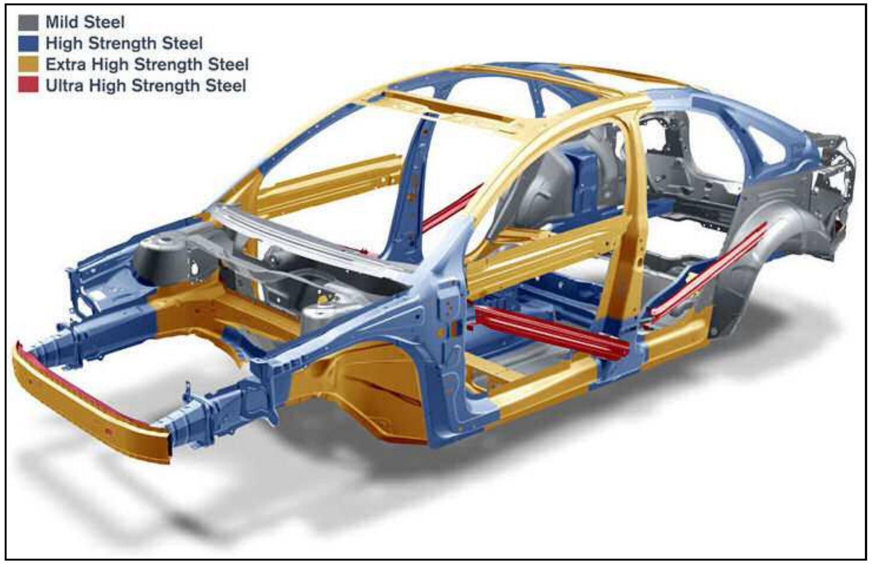

Industry annealing line before galvanizing

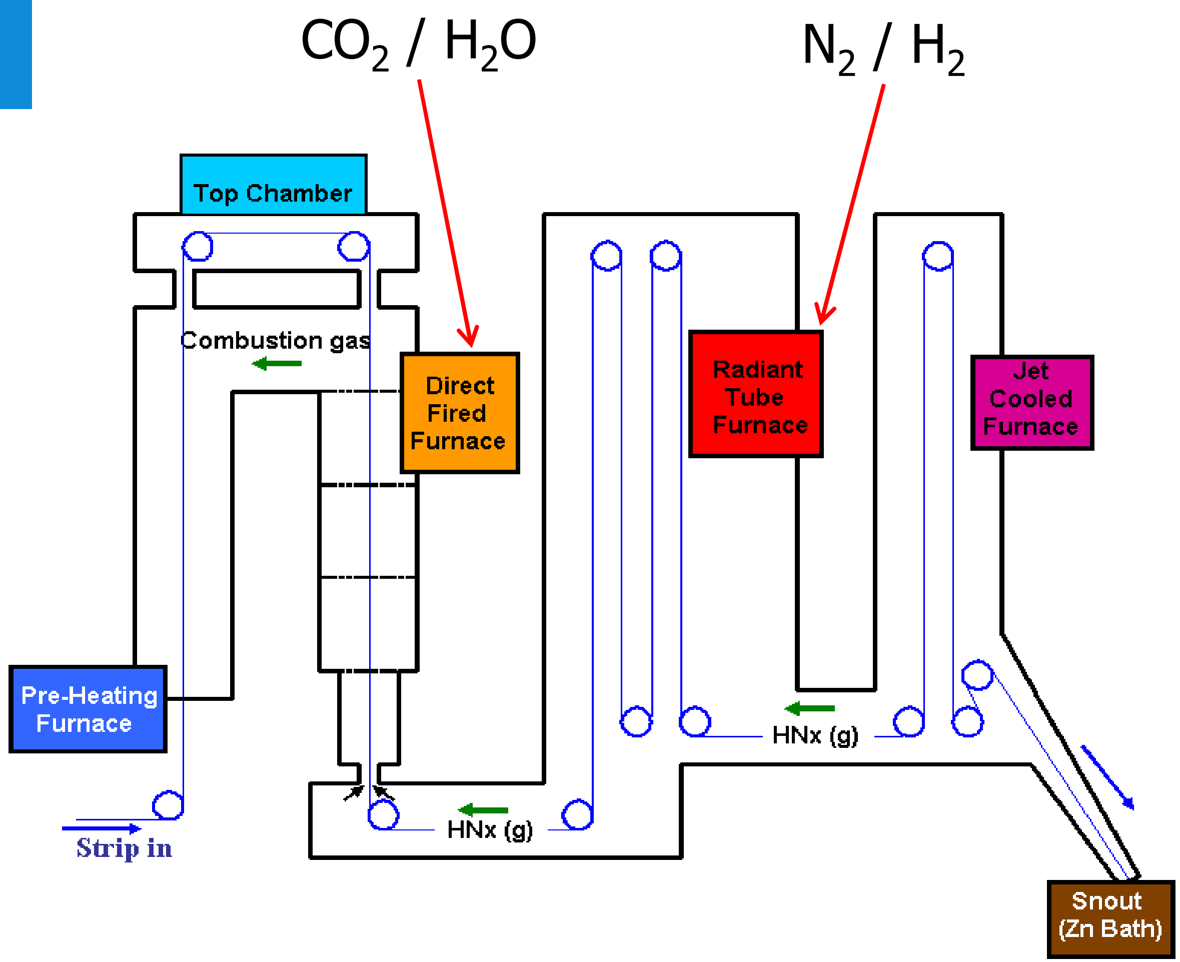

Oxidation environment in Direct Fired Furnace

Reduction atmosphere in Radiant Tube Furnace

Formation of oxides of alloying elements is thermodynamically favourable during annealing process

Problem of galvanizing quality

Major alloying element in AHSS: Mn, Si, Al, Cr

Poor adhesion of Zn coating due to stable oxides formed at steel surface

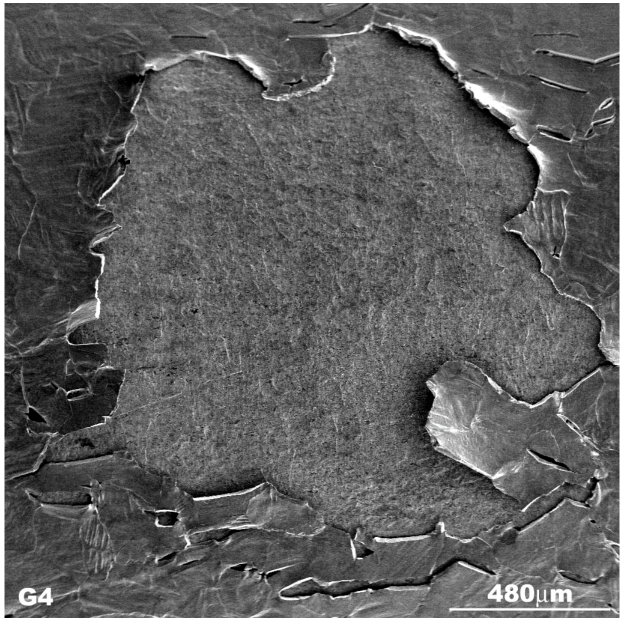

Goal: prevent external oxides formation

Project aim and industrial relevance

Aim:

- Development of oxidation model
- Predicting type of oxides formed
- Internal/external oxidation kinetics
- Final distribution of alloying elements

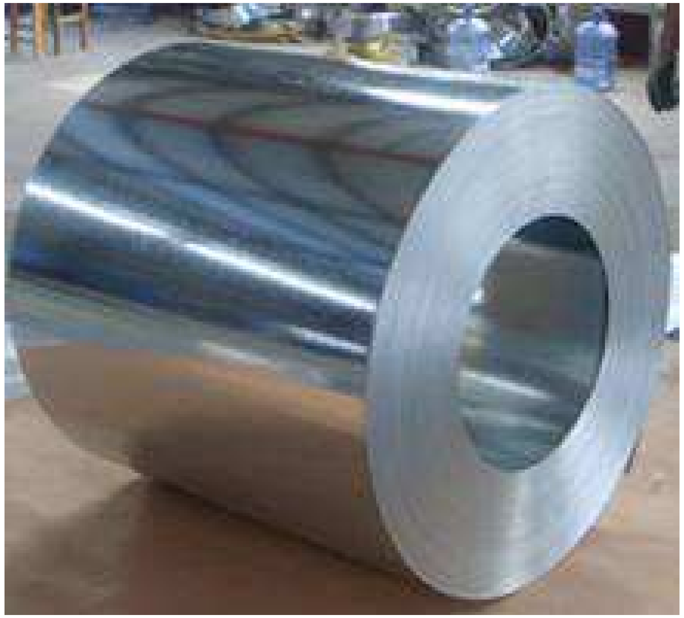

Relevance:

- Product development
  (e.g. alloying composition design)
- Process optimisation
  (e.g. annealing temperature, atmosphere)

2.

Prediction of oxide phases formed upon internal oxidation of Fe-Mn-Cr steels

Sample compositions

Steel composition in mole percent (weight percent in brackets)

Sample	C	Mn	Cr	Si	Al
Fe-1.7Mn	0.48 (0.10)	1.72 (1.70)	-	0.10 (0.05)	0.004 (0.002)
Fe-1.8Mn-0.5Cr	-	1.75 (1.72)	0.53 (0.49)	-	-
Fe-1.7Mn-1.5Cr	-	1.70 (1.67)	1.49 (1.39)	-	-
Fe-1.8Mn-0.6Cr-0.5Si	0.46 (0.10)	1.82 (1.80)	0.57 (0.53)	0.49 (0.25)	0.006 (0.003)
Fe-1.8Mn-1.1Cr-0.5Si	0.47 (0.10)	1.82 (1.80)	1.09 (1.02)	0.51 (0.26)	0.039 (0.019)
Fe-1.9Mn-1.0Cr-0.1Si	0.46 (0.10)	1.90 (1.88)	0.97 (0.91)	0.12 (0.06)	0.053 (0.026)
Fe-1.9Mn-1.6Cr-0.1Si	0.46 (0.10)	1.85 (1.83)	1.63 (1.53)	0.10 (0.05)	0.049 (0.024)
Fe-2.8Mn-0.6Cr-0.5Si	0.47 (0.10)	2.83 (2.80)	0.59 (0.55)	0.49 (0.25)	0.010 (0.005)

Effect of Cr and Si concentration can be studied

Annealing parameters

- Temperature: 950 ℃
  Measured by thermocouple inside the quartz tube
- Gas atmosphere: Ar/N_2 + 5 vol.% H_2
  5N quality of gas supply, subsequently, oxygen, moisture and hydrocarbon filtered (Messer Griesheim)
- Dew point (DP): -45, -37, -30, -10, and +10 ℃
  De-aerated water supply with dissolved O_2 less than 100 ppb
  Dew point measured by calibrated easidew and optidew (Michell Instruments)
- Annealing time: 1 hour

$$H_2O = H_2 + 1/2O_2 \qquad \frac{1}{2}\log pO_2 = 3 - \frac{13088}{T} + \log\left(\frac{pH_2O}{pH_2}\right)$$

Identification of oxide phases

X-ray diffraction (XRD) with grazing incidence geometry

Bruker D8 PSI

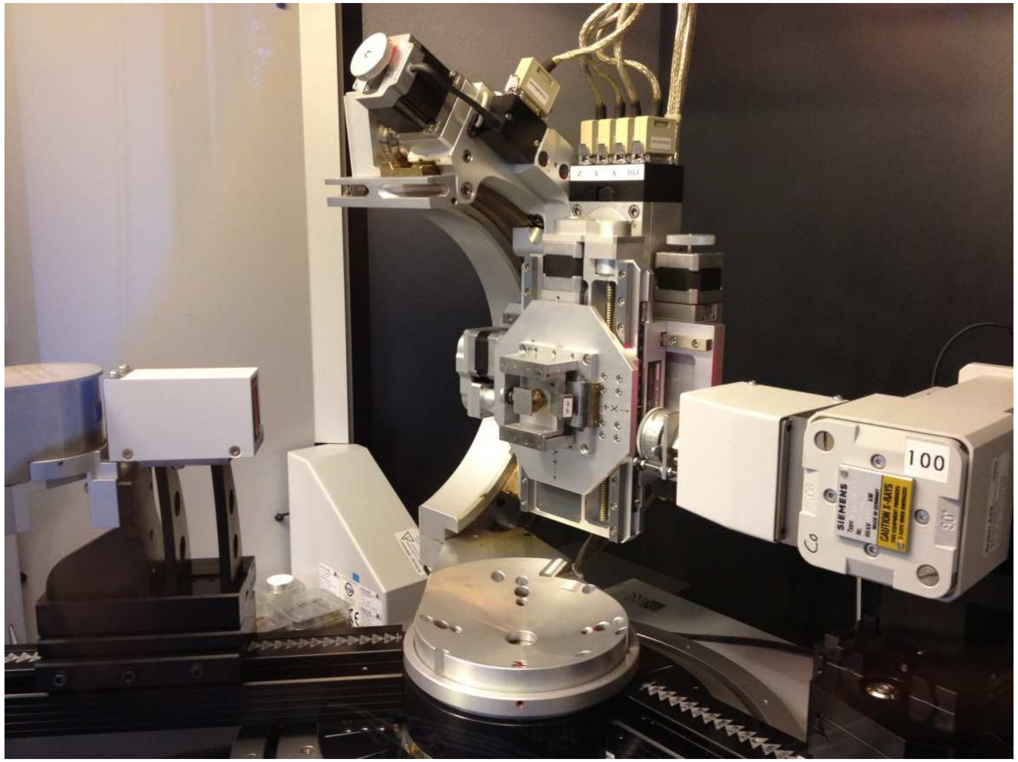

Grazing incidence detector scan

Co Kα radiation

Incident beam angle: 3°

2θ range: 20-60°

Analysis depth: 1.3 μm (70%)

Step size: 0.03° 2θ

Counting time per step: 10 seconds

SEM observation of oxidized samples

Annealing condition in N_2 with 5 vol.% H_2

Dew point (°C)	Temperature (°C)	pO_2
+10	950	2.3×10^{-17}

Sample composition (at.%):

C	Mn	Cr	Si	Al
0.47	1.82	1.09	0.51	0.039

Surface

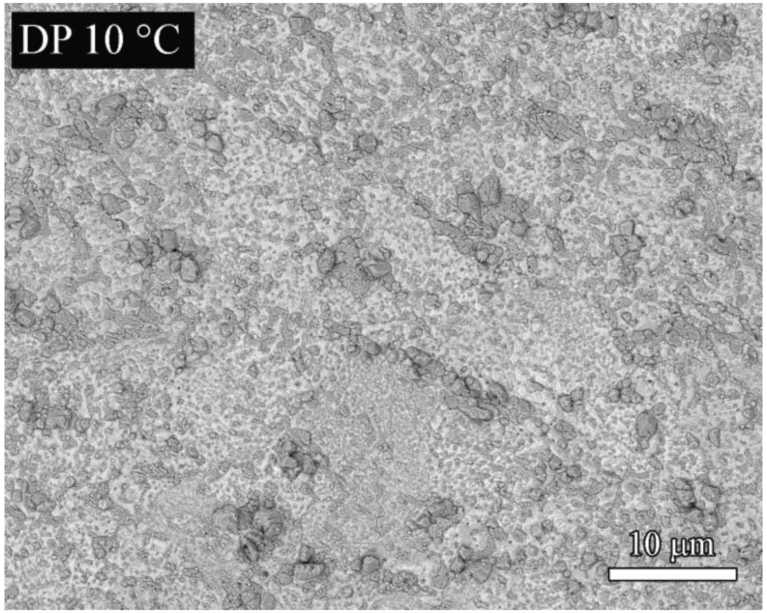

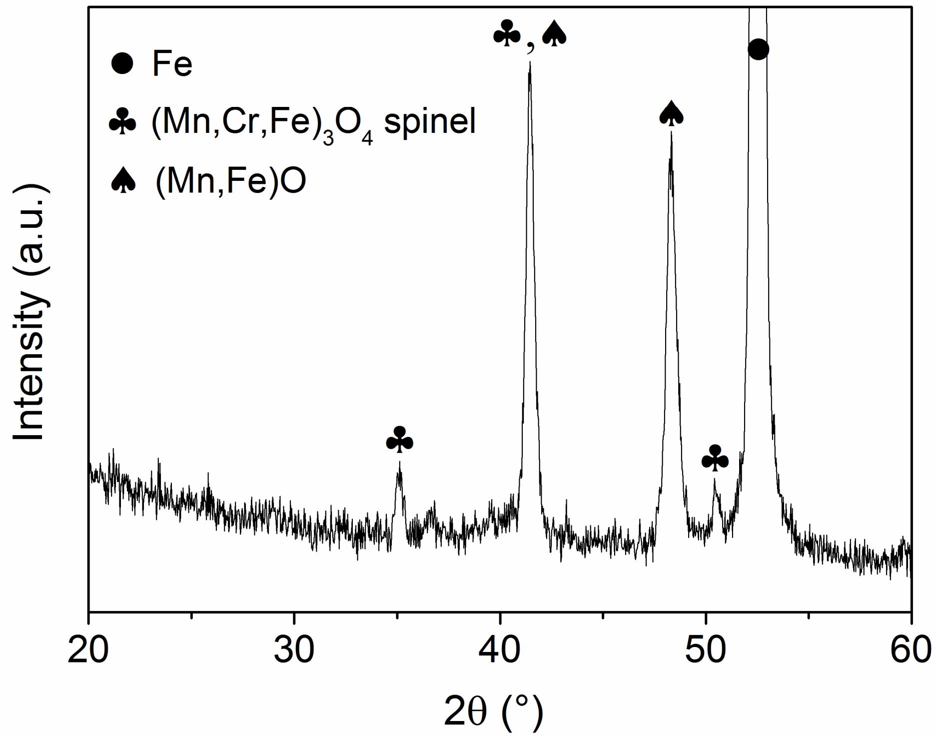

$(Mn,Cr,Fe)_3O_4$ and $(Mn,Fe)O$ form internally and at surface after annealing

Thermodynamics of oxide formation

Comparison of oxide phases with phase diagram

Fe-Mn binary alloys in oxidation environment at 950 ℃ computed with Factsage

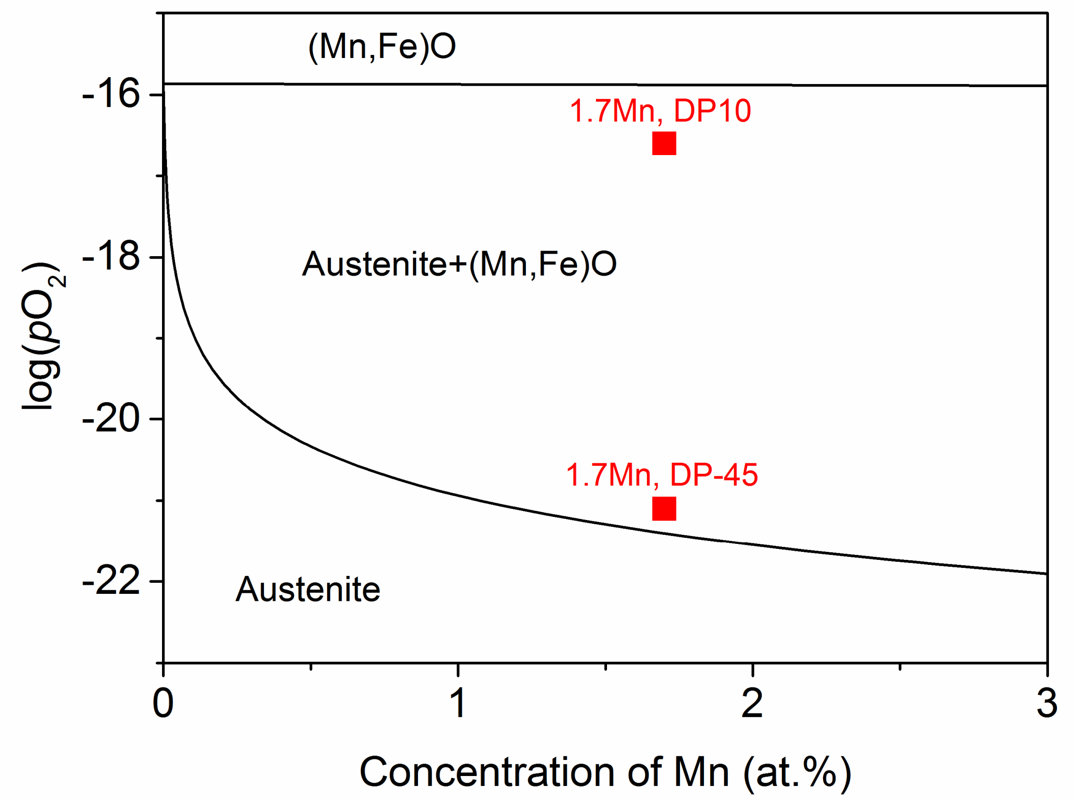

Database: FactPS, Ftoxid, FSstel

Solution phases selected in calculation: BSpinel, BMonoxide, AOlivine, Rhodonite, BCC_A2, FCC_A2

Compound species selected: SiO_2, Cr_2O_3 from Ftoxid

Gas phases selected: Ar, O_2 from FactPS

Dew point has no effect on type of oxides

Amount of Fe in (Mn,Fe)O increases with dew point

Observation in agreement with phase diagram

Thermodynamics of oxide formation

Effect of Cr on oxide formation in Fe-Mn steels

Fe – Cr -1.8 at.% Mn ternary alloys in oxidation environment at 950 ℃

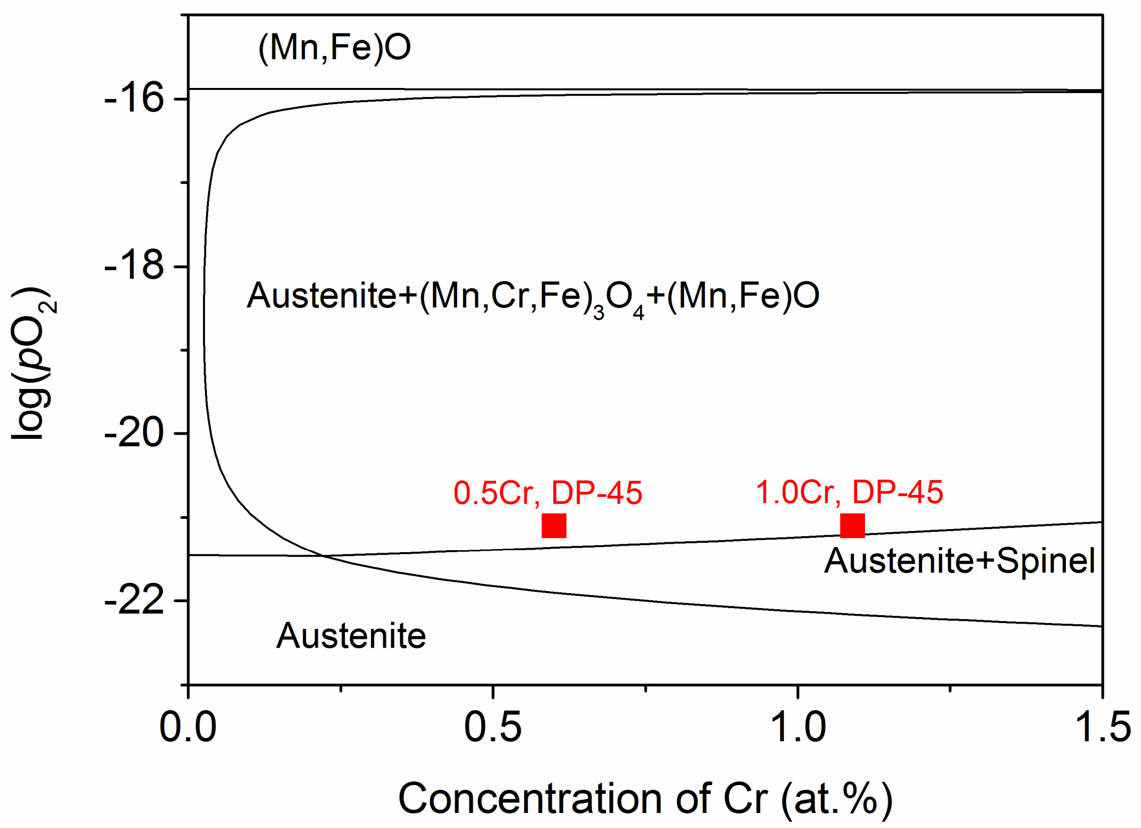

Adding Cr forms $(Mn,Cr,Fe)_3O_4$ spinel

Above 0.2 at.% Cr, dissociation pO_2 of (Mn,Fe)O is higher than $(Mn,Cr,Fe)_3O_4$

Dissociation pO_2 of (Mn,Fe)O increases with Cr concentration

Sample	DP-45	DP-37
Fe-1.8Mn-0.5Cr	$(Mn,Cr,Fe)_3O_4$ (Mn,Fe)O	-
Fe-1.7Mn-1.5Cr	$(Mn,Cr,Fe)_3O_4$	$(Mn,Cr,Fe)_3O_4$ (Mn,Fe)O
Fe-1.9Mn-1.0Cr-0.1Si	$(Mn,Cr,Fe)_3O_4$	$(Mn,Cr,Fe)_3O_4$ (Mn,Fe)O
Fe-1.9Mn-1.6Cr-0.1Si	$(Mn,Cr,Fe)_3O_4$	$(Mn,Cr,Fe)_3O_4$ (Mn,Fe)O

Observation in agreement with phase diagram

Thermodynamics of oxide formation

Effect of Si on oxide formation in Fe-Mn-Cr steels

Fe – Cr - 0.5 at.% Si - 1.8 or 2.8 at.% Mn quarternary alloys in oxidation environment at 950 ℃

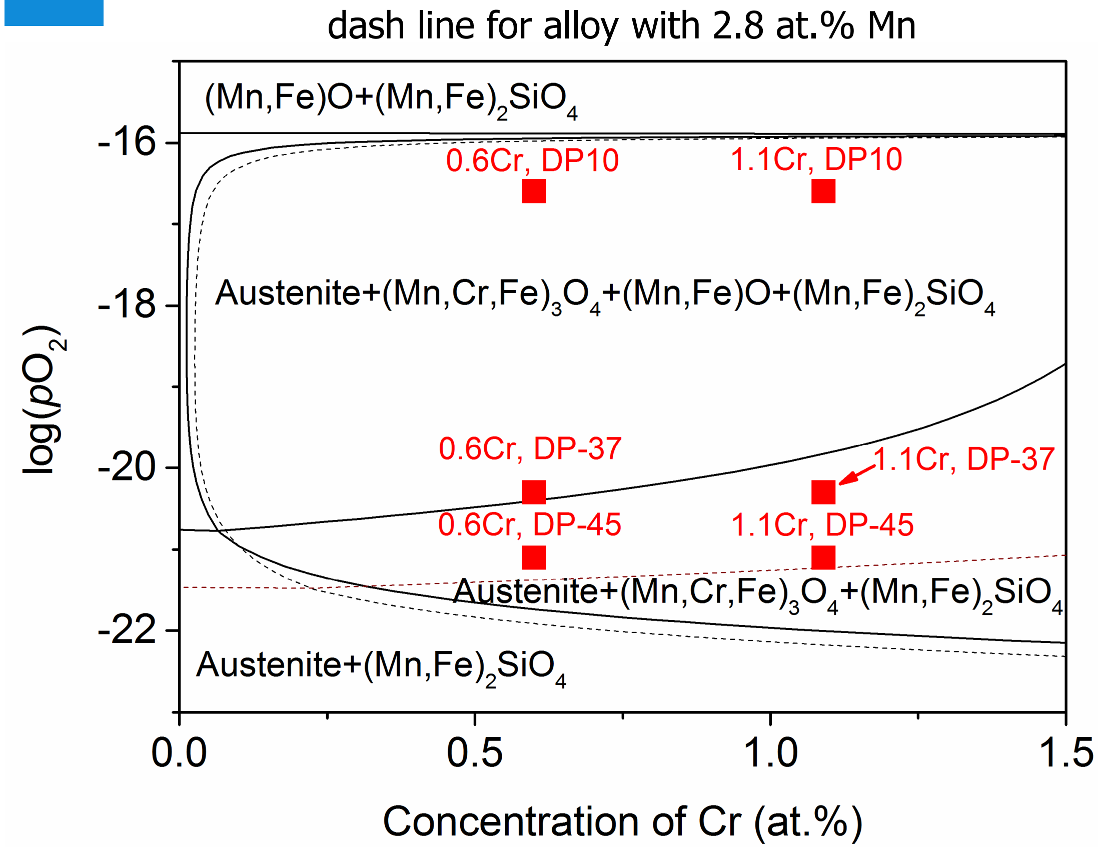

Adding Si forms $(Mn,Fe)_2SiO_4$ and dissociaiton pO_2 of $(Mn,Fe)_2SiO_4$ is lower than $(Mn,Cr,Fe)_3O_4$

Adding Si increases dissociation pO_2 of (Mn,Fe)O

Dissociation pO_2 of (Mn,Fe)O decreases with Mn concentration

Sample	DP-45	DP-37
Fe-1.8Mn-0.6Cr-0.5Si	$(Mn,Fe)_2SiO_4$	$(Mn,Cr,Fe)_3O_4$ $(Mn,Fe)_2SiO_4$
Fe-1.8Mn-1.1Cr-0.5Si	$(Mn,Fe)_2SiO_4$	$(Mn,Cr,Fe)_3O_4$ $(Mn,Fe)_2SiO_4$
Fe-1.9Mn-1.0Cr-0.1Si	$(Mn,Cr,Fe)_3O_4$	$(Mn,Cr,Fe)_3O_4$ (Mn,Fe)O
Fe-2.8Mn-0.6Cr-0.5Si	$(Mn,Cr,Fe)_3O_4$ (Mn,Fe)O $(Mn,Fe)_2SiO_4$	-

Adding Si suppress formation of $(Mn,Cr,Fe)_3O_4$

Thermodynamics of oxide formation

Effect of temperature and crystal lattice of alloy matrix

Fe - Cr - 0.5 at.% Si - 1.8 at.% Mn quarternary alloys in oxidation environment

850 ℃, dash line for austenite matrix

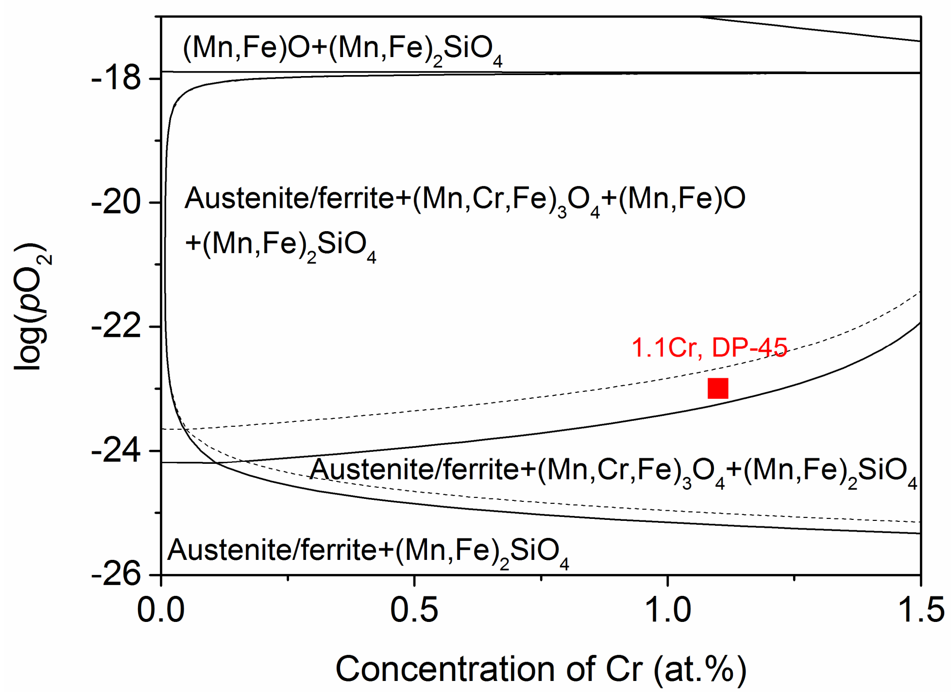

750 ℃

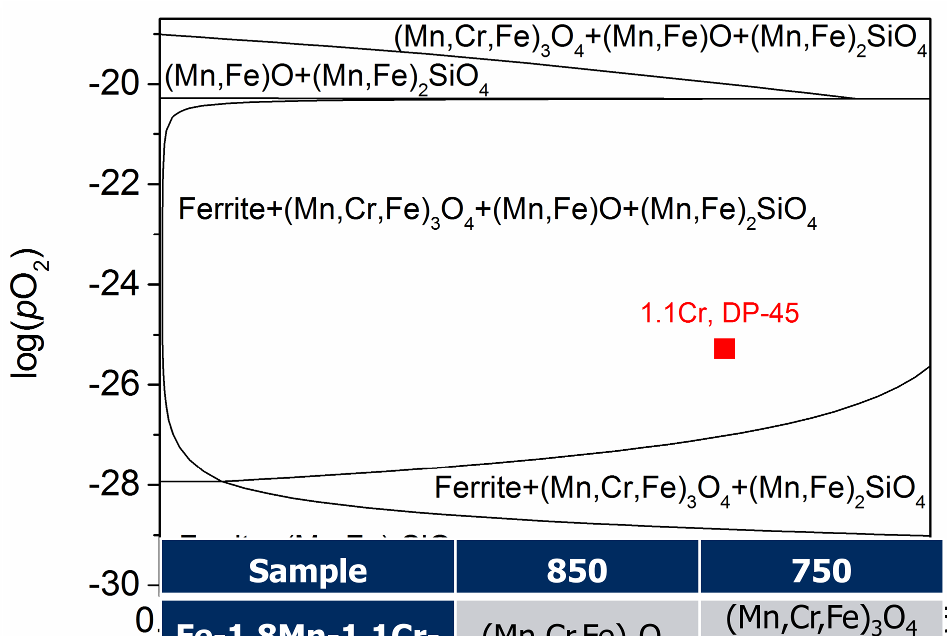

Sample	850	750
Fe-1.8Mn-1.1Cr-0.5Si	$(Mn,Cr,Fe)_3O_4$ $(Mn,Fe)_2SiO_4$	$(Mn,Cr,Fe)_3O_4$ $(Mn,Fe)O$ $(Mn,Fe)_2SiO_4$

Dissociation pO_2 of $(Mn,Cr,Fe)_3O_4$ and (Mn,Fe)O decreases with temperature

Dissociation pO_2 of $(Mn,Cr,Fe)_3O_4$ and (Mn,Fe)O in austenite is slightly higher than in ferrite

3.

Compositional depth profile of internal (Mn,Fe)O in oxidized Mn alloyed steel

W. Mao & W.G. Sloof, Scripta Materialia, 2017, vol. 135, pp 29-32.

Phase diagrams of Fe-1.7Mn alloy in oxidizing environment

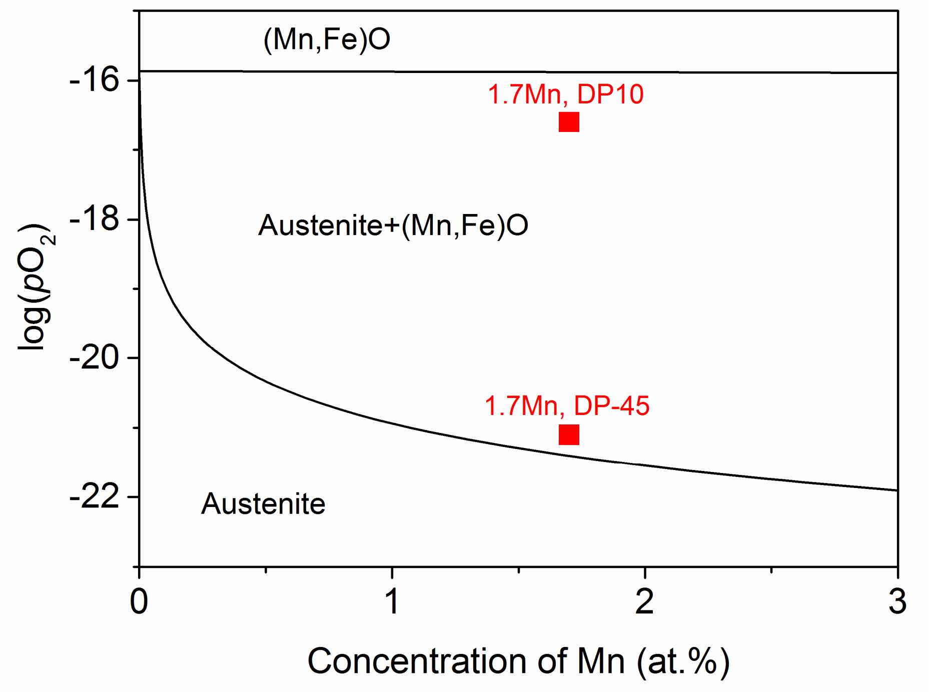

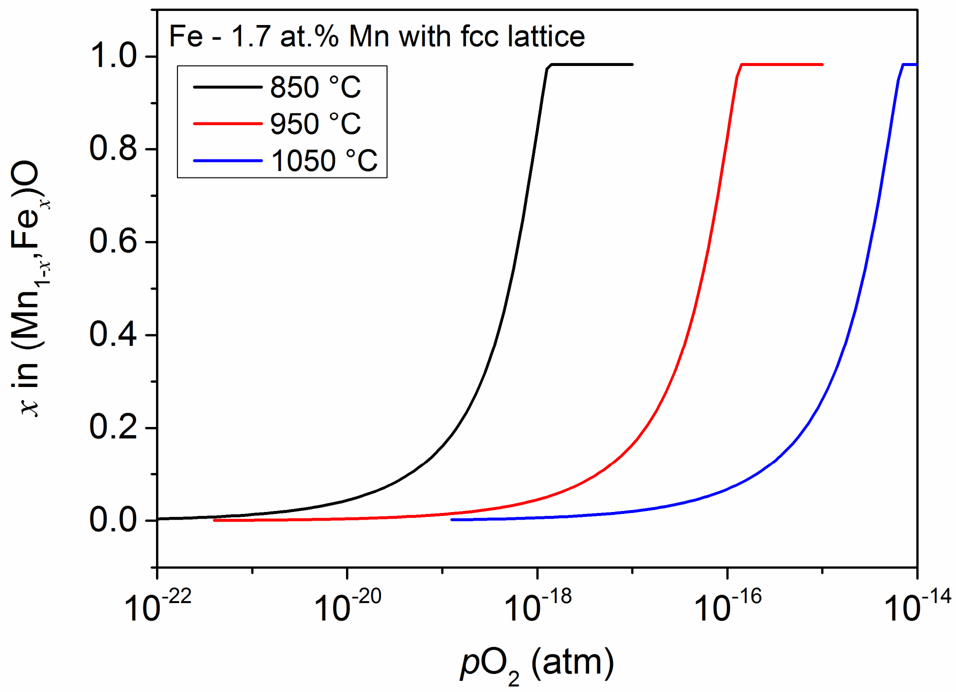

Fe concentration in (Mn,Fe)O increases with oxygen partial pressure

Predicted depth profile of internal oxidation zone

Annealing condition in N_2 with 5 vol.% H_2

Dew point (℃)	Temperature (℃)	pO_2
+10	950	2.3×10^{-17}

Sample composition (at.%):

C	Mn	Si	Al
0.48	1.72	0.097	0.004

$$N_{\underline{O}} = K_S (pO_2)^{1/2} \qquad K_S(950C) = 740$$

IOZ of Mn steel annealed for 1 hour

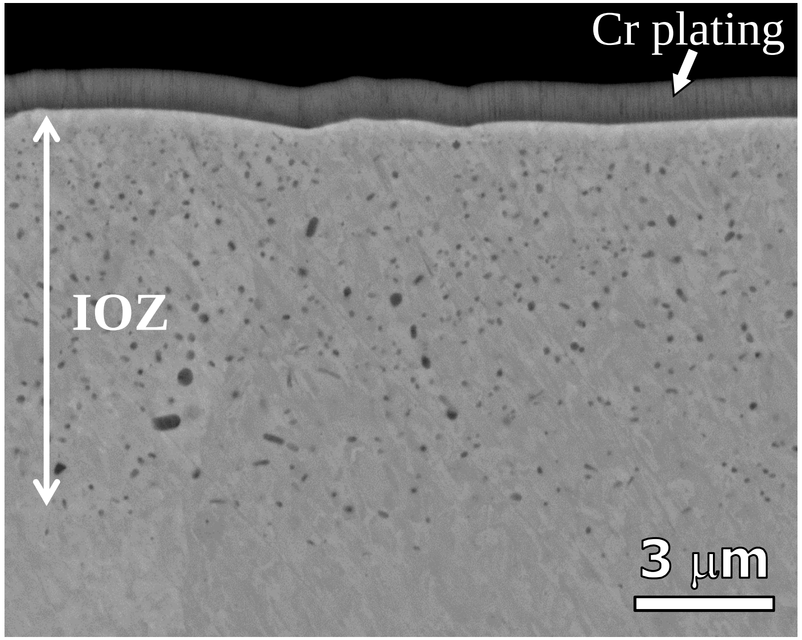

Simulated depth profile of dissolved O

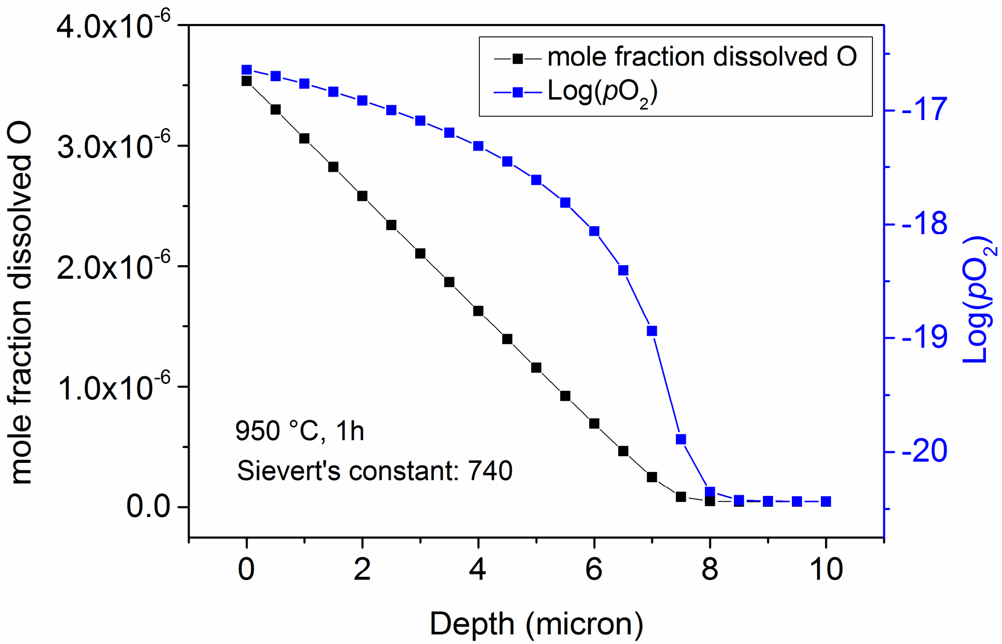

Activity of dissolved oxygen decreases with depth in internal oxidation zone

Predicted depth profile of internal oxidation zone

Annealing condition in N_2 with 5 vol.% H_2

Dew point (℃)	Temperature (℃)	pO_2
+10	950	2.3×10^{-17}

Sample composition (at.%):

C	Mn	Si	Al
0.48	1.72	0.097	0.004

Computed compositional depth profile of internal (Mn,Fe)O in Mn steels annealed for 1 hour

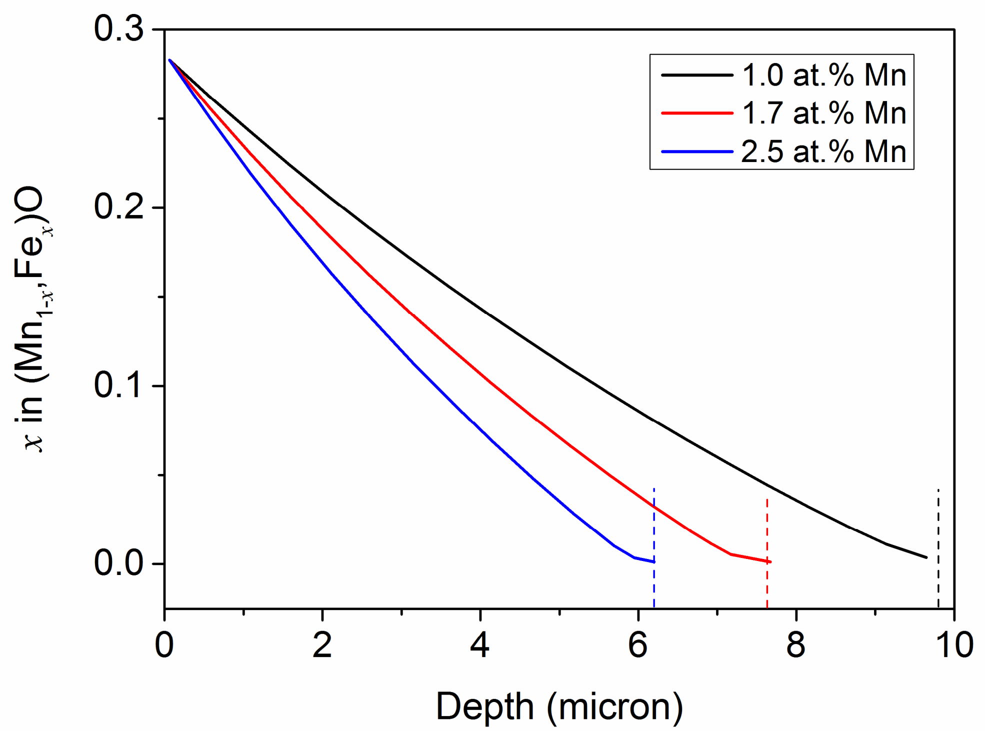

Fe concentration in (Mn,Fe)O as a function of pO_2 is computed with thermodynamic tool Factsage

Fe concentration in internal (Mn,Fe)O decreases with depth at thermodynamic equilibrium

Sample preparation

- Removal of surface layer by mechanical polishing
- Measured weight loss to determine thickness of removed surface layer

SEM surface observation and XPS spectrum after removing 1.4 μm of surface layer

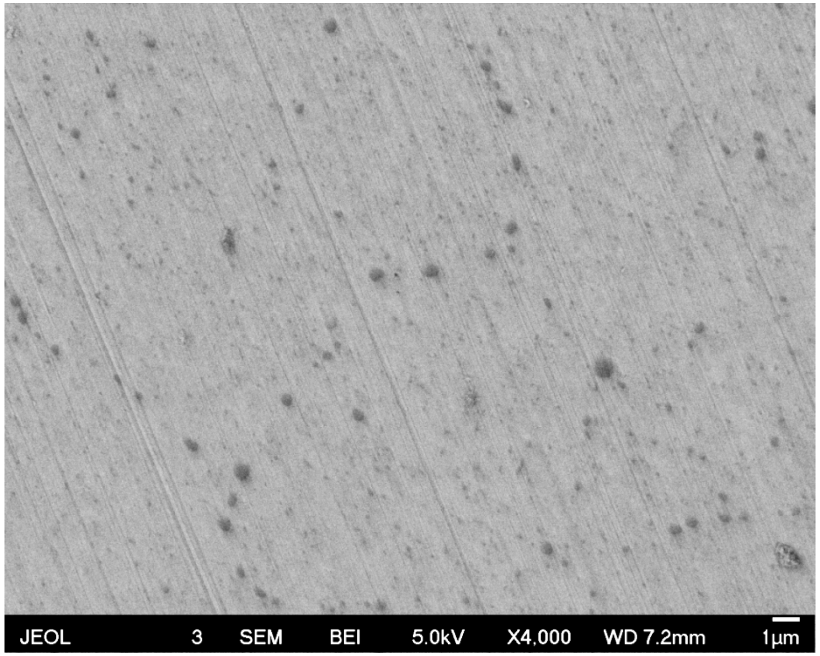

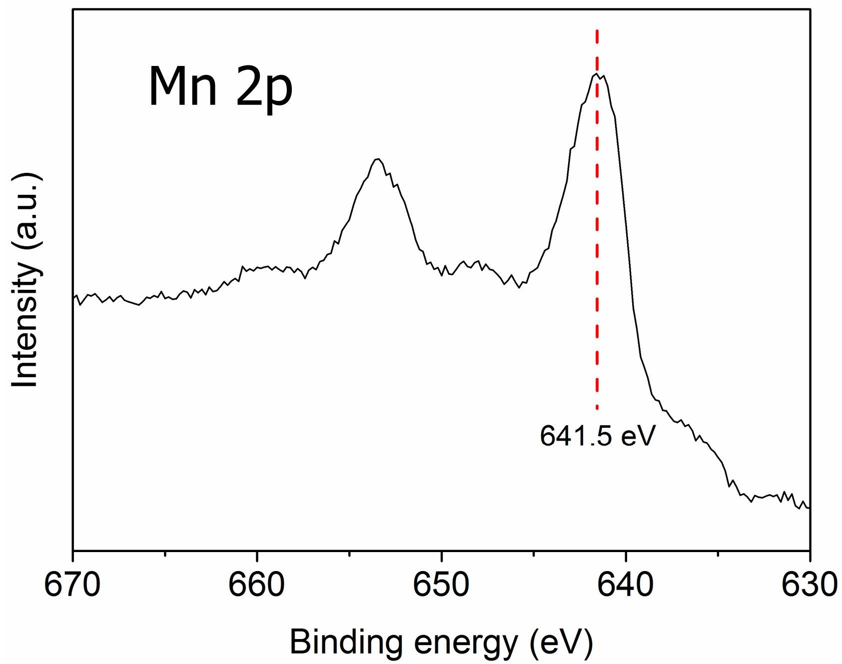

Mn 2p binding energy shifted indicating formation of intennal MnO

Measurement of (Mn,Fe)O composition

XRD patterns of (Mn,Fe)O formed in Fe – 7 wt.% Mn steel annealed at 950 °C from DP -45 to 10 °C

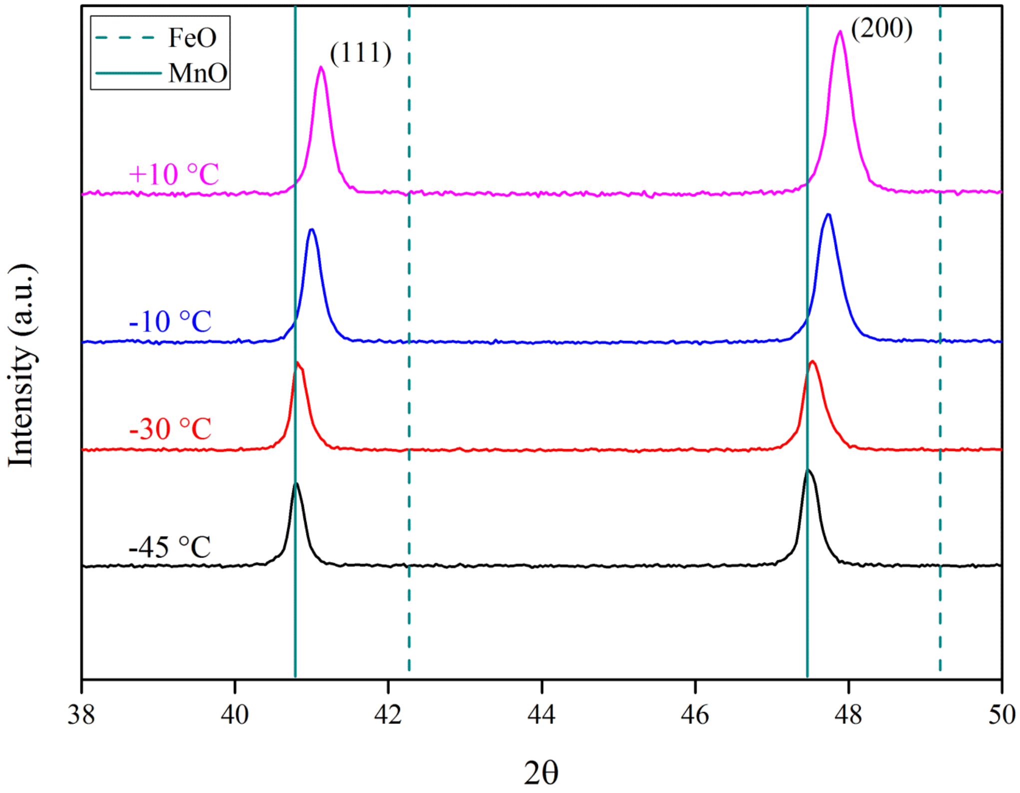

Diffraction peaks of (Mn,Fe)O shifted with increasing Fe concentration

Fe concentration in (Mn,Fe)O can be determined using Vagard's law

Depth profile of internal oxidation zone

Annealing condition in N_2 with 5 vol.% H_2

Dew point (˚C)	Temperature (˚C)	pO_2
+10	950	2.3×10^{-17}

Sample composition (at.%):

C	Mn	Si	Al
0.48	1.72	0.097	0.004

Comparison between prediction and experiment result

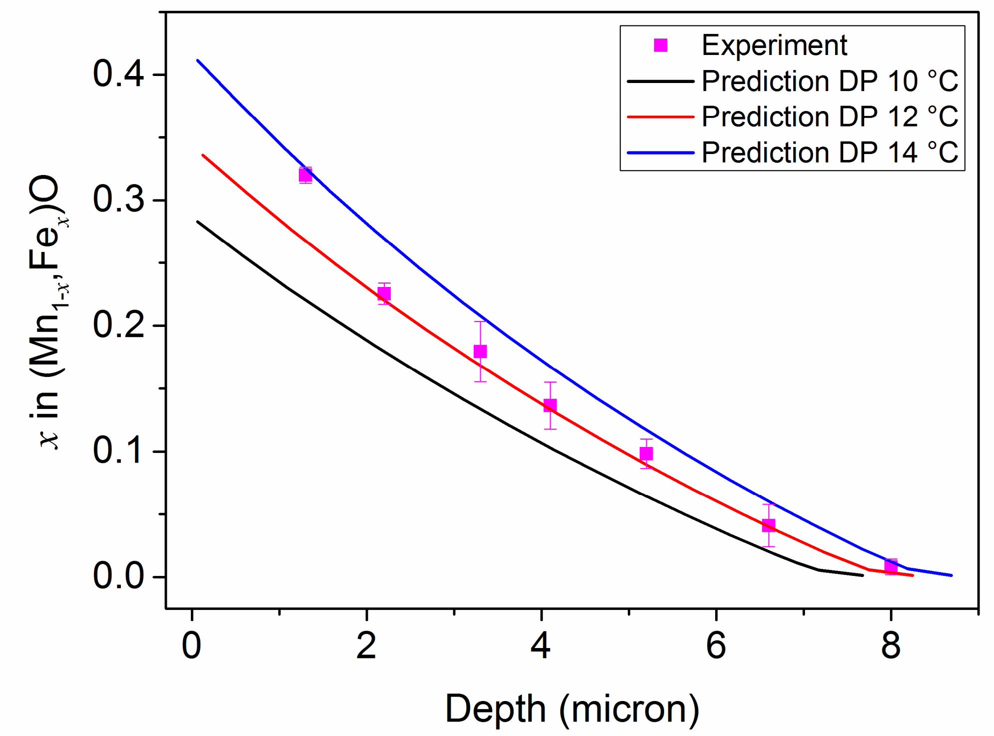

Fe concentration in (Mn,Fe)O precipitates decreases with depth

Measured compositional depth profile of internal (Mn,Fe)O in agreement with prediction

At each depth oxide precipitate is in thermodynamic equilibrium with dissolved oxygen

Summary

- Type of oxide phases formed during annealing of Mn, Cr and Si alloyed steels (AHSS) can be well predicted with thermodynamic tool Factsage

- Composition of oxide solution (e.g. (Mn,Fe)O) as a function of pO_2 can be well predicted with Factsage

- Thermodynamic data of Fe alloys in Fstel database and oxides in Ftoxid database are reliable, and can be applied for numerical simulation of internal oxidation behaviour of AHSS

Outlook

- Thermodynamic data of Fe-O-X ternary system in solid solution
- Coupling Factsage with other program (e.g. Matlab)